Charge Transfer between Alkali-Metal Ions and Cesium Atoms*

LAWRENCE L. MARINO†
Space Science Laboratory, General Dynamics, Convair, San Diego, California
(Received 14 June 1966)

The cross sections for charge transfer between alkali-metal ions and cesium atoms have been determined as a function of primary ion beam energy from 50 to 4500 eV. In all cases, structure consisting of oscillations whose amplitudes increased with primary ion beam energy was observed superimposed upon the normally expected form of the cross sections. Smith has shown that the cesium resonance results follow from the assumption that the difference between the even and odd eigenenergies ($V_g - V_u$) passes through an extremum. We find that the resonant cross section can be described by $Q(\text{cm}^2) = Q_0(\text{cm}^2) - A V^{1/4} \cos[\pi(|B|V^{-1/2} - \frac{1}{4})]$ where $A = 0.75 \times 10^{-16}$ cm^2 eV$^{-1/4}$, $B = -820$ eV$^{1/2}$, V is the ion beam energy, and Q_0 is the nonoscillating portion of the cross section. This expression results from the assumption that $V_g - V_u$ passes through a minimum of a negative function of internuclear distance. Potential parameters consistent with the quoted values of A and B are given. The nonresonant results can be fitted by the form $Q = Q_0 - A V^{1/4} \cos[\pi(|B|V^{-1/2} + \frac{1}{4})]$.

INTRODUCTION

THE previously determined cross section for charge transfer between rubidium ions and cesium atoms[1] indicated the presence of structure at about 2800 eV. Perel *et al.*[2] subsequently confirmed this result and, in addition, reported several oscillations for rubidium-ion energies in excess of 2800 eV. They also reported structure in the cesium-ion, cesium-atom cross section occurring at energies greater than those covered by Marino *et al.*[3] Using a slightly different experimental technique, we have remeasured our previously reported cross sections, and find oscillations whose amplitudes decrease as the ion beam energy decreases. These oscillations are within the uncertainties of the previous data except for the rubidium-ion, cesium-atom peak at 2800 eV. Structure observed in the remaining alkali-metal ion, cesium-atom cross sections is also reported. Smith[4] has shown that the resonant cross section can be explained by assuming that the difference in energy between the *gerade* and *ungerade* states possesses an extremum.

EXPERIMENT

Since the experimental arrangement has been presented previously,[3] only a general description will be given here. Primary ions were accelerated, mass-analyzed, and focused into the charge-transfer chamber. This chamber contained thermal cesium atoms. Their number density was measured by surface-ionizing those atoms effusing from an aperture system of known geometry located in the side of the chamber. The cesium-atom pressure was varied from 5×10^{-6} to 5×10^{-5} mm by controlling the temperature of the chamber. The charge of cesium was introduced by crushing, in vacuum, an ampoule contained in a reservoir connected to the chamber. Slow ions resulting from charge transfer over a known path length were measured by a pair of parallel, guarded plates to which suitable potentials were applied. The fast primary ion beam current was also determined.

In the previous work, the absolute cross section at a given ion beam energy was computed from a plot of slow-ion current per fast-ion current as a function of atom density. The present data were obtained by varying the primary ion beam energy at a fixed atom density. The charge-transfer chamber required several hours to stabilize at a given temperature, but after equilibrium was reached, relative cross sections were taken by varying the primary ion beam energy in 10-V increments. Data were taken with at least two different pressures in the charge-transfer chamber and with scale factors greater than unity so that structure could be more readily observed. The relative cross sections were normalized to absolute values, obtained by the method outlined above, and the mean then obtained. The relative data were taken by modifying a Leeds and Northrup recorder so that the reference

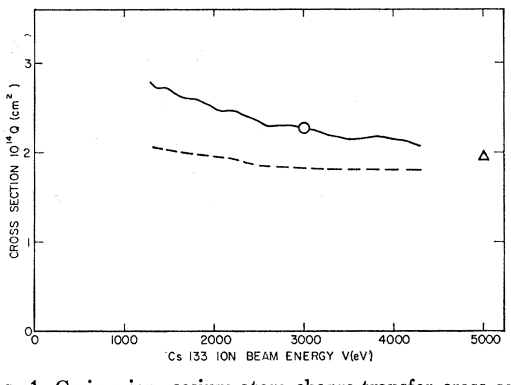

FIG. 1. Cesium-ion, cesium-atom charge-transfer cross section as a function of primary ion beam energy. The solid curve is the present result while the dashed curve is taken from Ref. 2. The circle at 3000 eV denotes the normalization point. The triangle is the corrected (see Ref. 3) result of D. V. Chkuaseli, U. D. Nikoleishvili, and A. I. Guldamashvili, Bull. Acad. Sci. U.S.S.R. **24**, 972 (1960).

* A preliminary report of this work appeared in Bull. Am. Phys. Soc. **11**, 733 (1966).

† Present address: Lawrence Radiation Laboratory, University of California, Livermore, California.

[1] L. L. Marino, in *Atomic Collision Processes*, edited by M. R. C. McDowell (North-Holland Publishing Company, Amsterdam, 1964), p. 807.

[2] J. Perel, R. H. Vernon, H. L. Vernon, and H. L. Daley, Phys. Rev. **138**, A937 (1965).

[3] L. L. Marino, A. C. H. Smith, and E. Caplinger, Phys. Rev. **128**, 2243 (1962).

[4] F. J. Smith, Phys. Letters **20**, 271 (1966).

voltage was obtained from the primary ion beam current; thus the ratio of slow ion current per unit primary ion current could be directly recorded.

The source of primary ions was of the aluminosilicate type.[5–8] A mixture consisting of one part (by molecular proportion) of alkali-metal carbonate, one part of aluminum oxide, and two parts of silicon dioxide was prepared. Amyl acetate was used to form a slurry and the mixture ground with a mortar and pestle. The compound was then painted on a platinum gauze about 1-cm square. The gauze was heated in vacuum by passing current directly through it. After an initial period during which carbon dioxide was given off, a stable alkali-metal ion beam was obtained. In the case of cesium, the nitrate was readily available rather than the carbonate and it also produced a satisfactory ion beam.

The results are presented in Figs. 1 through 5. Since the data points are so numerous, only the lines drawn through them are shown. For the most part the curves cover the points; however, at the larger primary beam energies where potential breakdown sometimes occurred, and at the smaller energies where current intensities were low, the scatter in some cases was greater than the width of the lines. For this reason, and because the oscillations are small and therefore subject to a certain amount of interpretation, a tabulation of the experimental points is available on request.

It is noted that the lithium-ion cesium-atom cross sections are very large. At a given velocity, this cross section is smaller than the others for low velocities, but rapidly rises to a value greater than that for the resonant process. Since a total cross section related to the collection of ions to a pair of parallel plates is measured, perhaps the large cross sections at the greater velocities reflect the contribution of other inelastic processes.

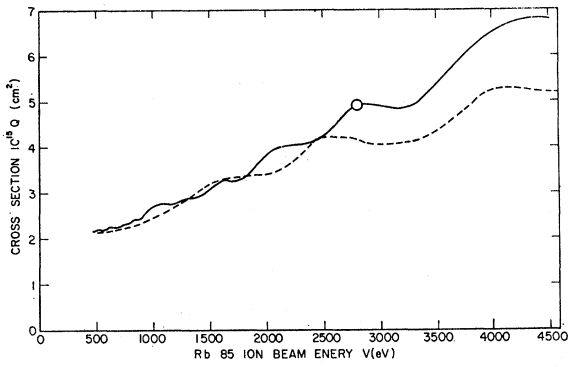

FIG. 2. Rubidium-ion, cesium-atom charge-transfer cross section as a function of primary ion beam energy. The solid curve is the present result with the circle at 2800 eV denoting the normalization point. The dashed curve is taken from Ref. 2.

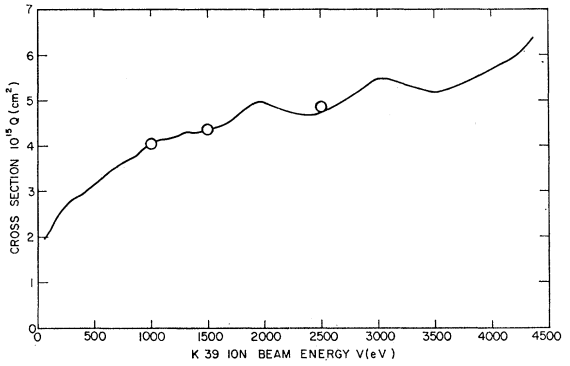

FIG. 3. Potassium-ion, cesium-atom charge-transfer cross section as a function of primary ion beam energy. The three circles were taken from a curve best fitting the absolute data reported by the author at the Fourth International Conference on the Physics of Electronic and Atomic Collisions, Quebec, Canada, 1965. The solid curve is the present result and was normalized to the circle at 1000 eV.

[5] S. K. Allison and M. Kamegai, Rev. Sci. Instr. **32**, 1090 (1961).
[6] J. P. Blewett and E. J. Jones, Phys. Rev. **50**, 464 (1936).
[7] K. T. Bainbridge, J. Franklin Inst. **212**, 317 (1931).
[8] J. L. Hundley, Phys. Rev. **30**, 864 (1927).

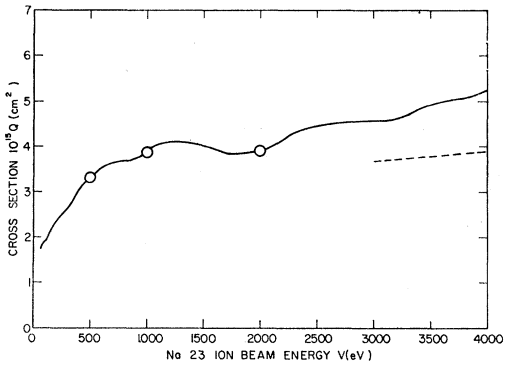

FIG. 4. Sodium-ion, cesium-atom charge-transfer cross section as a function of primary ion beam energy. The three absolute cross sections represented by the circles were obtained as part of this work. The solid curve was normalized to the circle at 500 eV. The slight curvature above 3300 eV is not predicted by theory and may not be real since all of the cross sections exhibited greater scatter at the higher energies. The dashed curve is the corrected result (see Ref. 3) of D. V. Chkuaseli, A. I. Guldamashvili, and U. D. Nikoleishvili, Bull. Acad. Sci. U.S.S.R. **27**, 976 (1963).

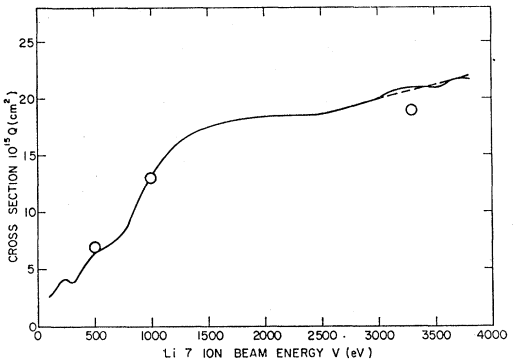

FIG. 5. Lithium-ion, cesium-atom charge-transfer cross section as a function of primary ion beam energy. The three circles are absolute cross sections obtained in the present work. The solid curve was normalized to the circle at 1000 eV. The solid curve above 3000 eV fits the data best while the dashed curve fits theory. It is noted that the scatter of the data is appreciably greater at these energies than for the remainder of the curve.

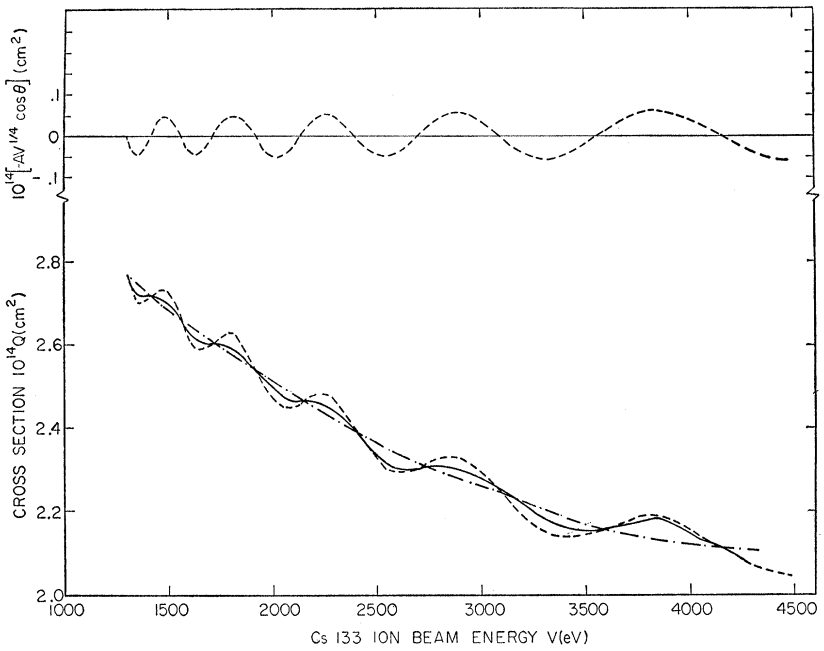

FIG. 6. Cesium-ion, cesium-atom cross section as a function of ion beam energy. The dashed curves are the results predicted by theory, the upper curve presenting only the oscillatory portion of the cross section. Q_0 (see text) is denoted by the dot-dash curve while the solid curve is the present result.

THEORY

The oscillations of a given collision pair occur at a constant reciprocal velocity interval. Further, the amplitudes increase with the velocity. Smith[4] has shown in the case of resonant charge-transfer collisions that these features result from a two-state approximation in which the difference between the *gerade* and *ungerade* potentials passes through an extremum.

The cross section can be represented in the two-state approximation by[9]

$$Q=\tfrac{1}{2}\pi\rho^2+2\pi\int_\rho^\infty b\sin^2\theta db, \tag{1}$$

where

$$\theta=\frac{1}{hv}\int_\rho^\infty\frac{r(V_g-V_u)dr}{(r^2-b^2)^{1/2}}=\frac{1}{hv}\eta(b). \tag{2}$$

Here v is the relative velocity, b is the impact parameter, and r is the internuclear distance, while V_g and V_u are the eigenergies of the *gerade* and *ungerade* states of the ion-atom molecule. The quantity $\frac{1}{2}\pi\rho^2$ can be determined in several ways. In the present work, it is not calculated but assigned to be the nonoscillatory part of the experimentally determined cross section.

TABLE I. Primary ion beam energies for which the oscillatory portion of the cesium-ion, cesium-atom cross section reaches maximum (V_M), minimum (V_m), and zero (V_z) values.

M	V_M (eV)	m	V_m (eV)	z	V_z (eV)
7	12 800(13 500)[a]	8	9860(10 900)[a]	25	4150
9	7850(8030)[a]	10	6400(6350)[a]	27	3560
11	5300(5270)[a]	12	4480	29	3090
13	3820	14	3310	31	2710
15	2890	16	2550	33	2390
17	2260	18	2020	35	2140
19	1810	20	1640	37	1920
21	1490	22	1360	39	1720
				41	1560
				43	1420
				45	1300

[a] Reference 2.

Smith points out that if $\eta(b)$ possesses an extremum at $b=b_0$, the method of stationary phase[10] may be employed to approximate the value of the integral in Eq. (1). The specialized form that is required here is

$$\int_\alpha^\beta g(b)e^{ixk(b)}db+\int_\alpha^\beta g(b)e^{-ixk(b)}db$$
$$=2(2\pi)^{1/2}[\pm k''(b_0)x]^{-1/2}g(b_0)\cos[xk(b_0)\pm\tfrac{1}{4}\pi] \tag{3}$$

for large x, where the plus (minus) sign is appropriate to a minimum (maximum) in $\eta(b)$ at $b=b_0$, and $k''(b_0)$ indicates the second derivative of k with respect to b evaluated at the extremum point $b=b_0$. Thus,

$$Q=\tfrac{1}{2}\pi\rho^2-\pi b_0(hv)^{1/2}[\pm 2\eta''(b_0)]^{-1/2}$$
$$\times\cos\{\pi[(4\eta(b_0)/hv)\pm\tfrac{1}{4}]\}. \tag{4}$$

This expression may be placed in the more convenient form

$$Q(cm^2)=Q_0(\text{cm}^2)-0.648\times10^{-16}b_0[\pm\eta''(b_0)]^{-1/2}$$
$$\times(V/M)^{1/4}\cos\{\pi[3.69(M/V)^{1/2}\eta(b_0)\pm\tfrac{1}{4}]\}, \tag{5}$$

where $Q_0=\frac{1}{2}\pi\rho^2$, b_0 is measured in units of a_0, $\eta(b_0)$ in a_0 eV, $\eta''(b_0)$ in eV/a_0, M is the primary ion mass number, and V is the primary ion energy in eV.

For cesium, Eq. (5) may be written as

$$Q=Q_0-AV^{1/4}\cos[\pi(BV^{-1/2}\pm\tfrac{1}{4})], \tag{6}$$

[9] D. R. Bates, in *Atomic and Molecular Processes*, edited by D. R. Bates (Academic Press Inc., New York, 1962), p. 602.

[10] A. Erdelyi, *Asymptotic Expansions* (Dover Publications, Inc., New York, 1956), p. 51.

where $B=42.5\eta(b_0)$ and $A=0.191\times10^{-16}b_0[\pm\eta''(b_0)]^{-1/2}$. The oscillatory portion of the cross section causes Q to reach a maximum at $B(V_M)^{-1/2}\pm\frac{1}{4}=\pm M$, $M=1, 3, 5, \cdots$, a minimum at $B(V_m)^{-1/2}\pm\frac{1}{4}=\pm m$, $m=0, 2, 4, \cdots$, and Q_0 at $B(V_z)^{-1/2}\pm\frac{1}{4}=\pm\frac{1}{2}z$, $z=1, 3, 5, \cdots$, where the plus (minus) sign of m, M, and z is to be taken for $\eta(b_0)$ greater (less) than zero. The cross section is seen to be periodic in $V_M^{-1/2}-V_{M+2}^{-1/2}=\Delta(V_M)^{-1/2}=\Delta(V_m)^{-1/2}=2\Delta(V_z)^{-1/2}=-2/|B|$.

Experimentally, for the case of cesium-ion, cesium-atom charge transfer, we find that $\Delta(V_M)^{-1/2}=-2.44\times10^{-3}$ $(\text{eV})^{-1/2}$. V_M, V_m, and V_z in Table I were computed from $V_M=64\{[\Delta(V_M)^{-1/2}](4M+1)\}^{-2}$, $V_m=64\{[\Delta(V_m)^{-1/2}](4m+1)\}^{-2}$, and $V_z=16\{[\Delta(V_z)^{-1/2}]\times(2z+1)\}^{-2}$ anticipating that $\eta(b_0)$ is a minimum of a negative function of b. Therefore $B=-820(\text{eV})^{1/2}$ and $\eta(b_0)=-19.3\ a_0$ eV.

The dependence of the variation of the amplitude of the oscillations with energy is difficult to ascertain because the oscillations are small. Since the averaging treatment of our data tends to reduce the amplitudes, and since the results of Perel *et al.*[2] were obtained at greater energies with consequently larger oscillations, these last-named data were used to assign a value of 0.75×10^{-16} $\text{cm}^2(\text{eV})^{-1/4}$ to A. Thus the form

$$Q(\text{cm}^2)=Q_0-0.75\times10^{-16}V^{1/4}\cos[\pi(820V^{-1/2}-\tfrac{1}{4})] \quad (7)$$

was used to obtain the theoretical cross section in Fig. 6. Q_0 is the cross section obtained by drawing a smooth curve through the points at energies V_z.

Smith constructed empirical potentials to reproduce the cesium resonance results of Ref. 2. By using one set of potentials similar in form to his long-range potentials together with the experimental data, A and B, it is possible to determine analytically some of the pertinent parameters. Letting $V_g=D_e\{\exp[-2\beta(r-r_e)]-2\exp[\beta(r-r_e)]\}$ and $V_u=\gamma\exp(-\delta r)$, Eq. (2) results in

$$\eta(b)=D_e e^{2\beta r_e}\int_\rho^\infty\frac{e^{-2\beta r}r\,dr}{(r^2-b^2)^{1/2}}-2D_e e^{\beta r_e}\int_\rho^\infty\frac{e^{-\beta r}r\,dr}{(r^2-b^2)^{1/2}}-\gamma\int_\rho^\infty\frac{e^{-\delta r}r\,dr}{(r^2-b^2)^{1/2}}. \quad (8)$$

These Weyl fractional integrals may be evaluated[11] to yield

$$\eta(b)=D_e e^{2\beta r_e}bK_1(2\beta b)-2D_e e^{\beta r_e}bK_1(\beta b)-\gamma bK_1(\delta b), \quad (9)$$

where K_1 is the first-order modified Bessel function of the second kind.[12] Also,

$$\eta'(b)=2\beta bD_e e^{\beta r_e}K_0(\beta b)+\gamma b\delta K_0(\delta b)-2\beta bD_e e^{2\beta r_e}K_0(2\beta b), \quad (10)$$

where $\eta'(b)$ indicates the first derivative with respect to b and K_0 is the zero-order modified Bessel function of the second kind.[12] At the extremum,

$$\gamma\delta K_0(\delta b_0)=2\beta e^{\beta r_e}D_e[e^{\beta r_e}K_0(2\beta b_0)-K_0(\beta b_0)]. \quad (11)$$

Further,

$$\eta''(b)=\gamma\delta K_0(\delta b)-2\beta e^{\beta r_e}D_e[e^{\beta r_e}K_0(2\beta b)-K_0(\beta b)]+4\beta^2D_e e^{2\beta r_e}bK_1(2\beta b)-2\beta^2D_e e^{\beta r_e}bK_1(\beta b)-\gamma\delta^2bK_1(\delta b), \quad (12)$$

and at $b=b_0$

$$\eta''(b_0)=4\beta^2D_e e^{2\beta r_e}b_0K_1(2\beta b_0)-2\beta^2D_e e^{\beta r_e}b_0K_1(\beta b_0)-\gamma\delta^2b_0K_1(\delta b_0). \quad (13)$$

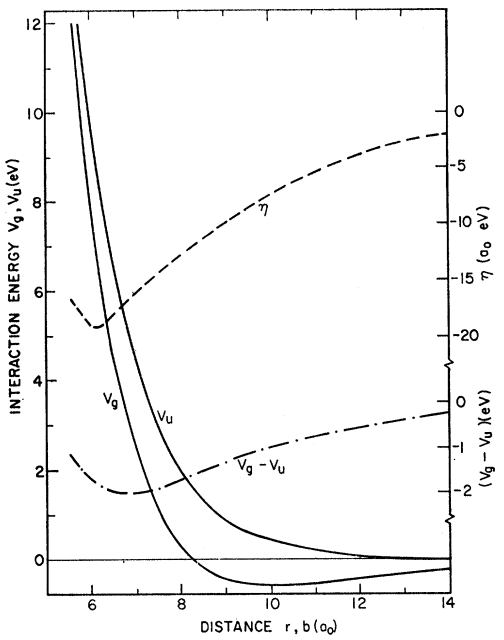

FIG. 7. This figure presents a possible set of parameters consistent with the experimental results. See Ref. 4 for a somewhat different set. The *gerade* and *ungerade* states are represented by V_g and V_u, respectively, while η is the integral appearing in Eq. (2) of the text. It is evident that an extremum in V_g-V_u implies an extremum in η.

TABLE II. Primary ion beam energies for which the oscillatory portion of the nonresonant cross sections reach maximum values. These energies were computed from the listed values of $\Delta[V(\text{eV})]^{-1/2}$ which were obtained from the data. V_m and V_z may also be readily computed.

Rb^+-Cs $\Delta(V)^{-1/2}=0.298\times10^{-2}$		K^+-Cs $\Delta(V)^{-1/2}=0.423\times10^{-2}$		Na^+-Cs $\Delta(V)^{-1/2}=0.840\times10^{-2}$		Li^+-Cs $\Delta(V)^{-1/2}=1.94\times10^{-2}$	
M	V_M (eV)	M	V_M (eV)	M	V_M (eV)	M	V_M (eV)
5	19 900 (23 300)[a]	9	2920	5	2510	3	1410
7	9870 (11 500)[a]	11	1930	7	1240	5	470
9	5870 (6320)[a]	13	1370	9	740	7	233
11	3890 (4130)[a]	15	1030				
13	2770 (2600)[a]	17	800				
15	2070						
17	1610						
19	1280						
21	1040						
23	870						
25	730						
27	630						
29	540						

[a] Reference 2.

[11] *Bateman Manuscript Project*, edited by A. Erdelyi (McGraw-Hill Book Company, Inc., New York, 1954), Vol. 2, p. 203.

[12] *Handbook of Mathematical Functions*, edited by M. Abramowitz and I. A. Stegun (Dover Publications, Inc., New York, 1965), pp. 374 and 417.

From Eqs. (9) and (13),

$$\delta^2\eta(b_0)-\eta''(b_0)=D_e e^{2\beta r_e}b_0K_1(2\beta b_0)[\delta^2-4\beta^2] -2D_e e^{\beta r_e}b_0K_1(\beta b_0)[\delta^2-\beta^2]. \quad (14)$$

From the expression for the amplitude, and with the experimental value $A=0.75\times10^{-16}$ cm^2(eV)$^{-1/4}$, the relation $\eta''(b_0)=0.0648\ b_0^2$ eV a_0^{-3} is obtained.

Using this value for $\eta''(b_0)$ and Smith's values of $D_e=0.56$ eV, $\delta=0.761/a_0$, $\beta=0.388/a_0$, and $r_e=10.1\ a_0$, Eq. (14) may be solved for $b_0=6.1\ a_0$. Also, γ may be calculated from Eq. (11) to be 927 eV and $\eta''(b_0)=2.41$ eV/a_0. V_g, V_u, (V_g-V_u), and η are shown in Fig. 7.

In the case of the nonresonant collision pairs, it is found that the cross sections can be fitted by $Q=Q_0-AV^{1/4}\cos[\pi(|B|V^{-1/2}+\frac{1}{4})]$. Within the formalism of the uncoupled equations resulting from the two-state treatment of resonant charge transfer, this would require making the not unreasonable assumption that a minimum of a positive function of $\eta(b)$ exists; however, no justification is provided for applying the theory to the nonresonant results. Values of M, V_M, and $\Delta(V)^{-1/2}$ for these collision pairs are given in Table II.

PHYSICAL REVIEW VOLUME 152, NUMBER 1 2 DECEMBER 1966

Excited-State Wave Functions, Excitation Energies, and Oscillator Strengths for Krypton and Xenon*

JOHN D. DOW AND ROBERT S. KNOX
Department of Physics and Astronomy, University of Rochester, Rochester, New York
(Received 11 May 1966)

Solutions of the nonrelativistic Hartree-Fock equations for ^3P and ^1P terms of the $np^5(n+1)s$ configurations and for the center of gravity of the np^5nd configurations of krypton ($n=4$) and xenon ($n=5$) have been obtained. Wave functions are tabulated and results of computations of excitation energies and oscillator strengths are presented. For krypton, the computed oscillator strengths of the 1165-Å and 1236-Å lines are 0.136 and 0.138, and for xenon those of the 1296-Å and 1470-Å lines are 0.147 and 0.194, respectively. Calculated values of various parameters such as spin-orbit interaction and excitation energies compare satisfactorily with experimental values. The adequacy of the nonrelativistic Hartree-Fock approximation is discussed.

1. INTRODUCTION

OSCILLATOR strengths for absorption to the low-lying (p^5s; $^1P_1$ and $^3P_1$) excited electronic states of atomic Kr and Xe have recently been measured,[1–3] prompting us to extend earlier calculations of Hartree-Fock functions for argon[4] and neon[5] to these heavier rare gases. The resulting nonrelativistic description of krypton and xenon appears to be quite accurate, as far as we can tell from computations of spin-orbit interaction, excitation energies, dipole matrix elements, decay times, static polarizabilities, and diamagnetic susceptibilities. Comparison is made with the experimentally measured values and with the results of previous calculations.[4–6]

In Sec. 2, the radial Fock equations are written, their solution is discussed, and abbreviated tables of radial wave functions are presented. Section 3 is concerned with electrostatic energies and spin-orbit parameters. Computed oscillator strengths, dipole matrix elements, decay times, and static polarizabilities are presented in Sec. 4. Section 5 briefly treats the interaction of the p^5d and p^5s configurations and includes a general discussion of the results.

2. HARTREE-FOCK EQUATIONS

A. Formulation

Shortley[7] has given a concise method for writing the Hartree-Fock equations[8] in the central-field approximation for configurations involving unfilled shells. We present his results, transcribed to atomic units, for the special case of configurations with one electron and one hole. We label the lone electron with the quantum numbers $n_e l_e m_e \sigma_e$; the quantum numbers associated with the electron missing from the almost-filled shell are $n_h l_h m_h \sigma_h$. The Hartree-Fock equations are

* Research supported by the U. S. Air Force Office of Scientific Research under Grant No. 611-64.
[1] D. K. Anderson, Phys. Rev. **137**, A21 (1965).
[2] J. Geiger, Z. Physik **177**, 138 (1963).
[3] P. G. Wilkinson, J. Quant. Spectr. Radiative Transfer **5**, 503 (1965).
[4] R. S. Knox, Phys. Rev. **110**, 375 (1958).
[5] A. Gold and R. S. Knox, Phys. Rev. **113**, 834 (1959).
[6] J. W. Cooper, Phys. Rev. **128**, 681 (1962).
[7] G. H. Shortley, Phys. Rev. **50**, 1072 (1936).
[8] D. R. Hartree, Proc. Cambridge Phil. Soc. **24**, 89 (1928); V. Fock, Z. Physik **61**, 126 (1930). For recent developments and standard notation, see D. R. Hartree, *The Calculation of Atomic Structures* (John Wiley & Sons, Inc., New York, 1957).